Journal of Materials Chemistry C

Accepted Manuscript

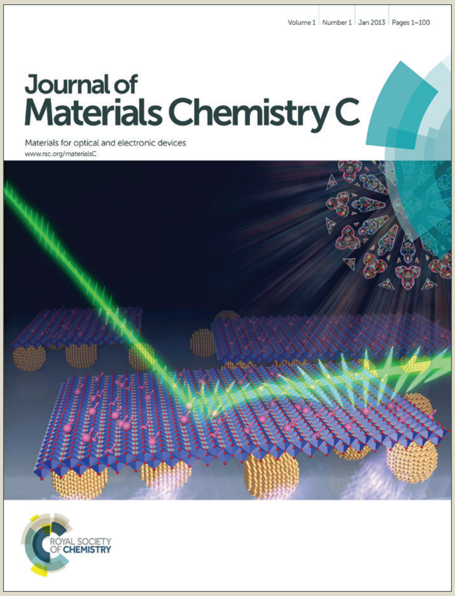

ROYAL SOCIETY OF CHEMISTRY

www.rsc.org/materialsC

Journal of Materials Chemistry C

Dynamic Article Links ►

Cite this: DOI: 10.1039/c0xx00000x

www.rsc.org/xxxxxx

COMMUNICATION

Unusually high SCLC hole mobility in solution-processed thin films of a polycyclic thiophene-based small-molecule semiconductor†

Yong Li,[a] Robert G. Clevenger,[a] Lu Jin,[a] Kathleen V. Kilway*[a] and Zhonghua Peng*[a]

Received (in XXX, XXX) Xth XXXXXXXXX 20XX, Accepted Xth XXXXXXXXX 20XX

DOI: 10.1039/b000000x

SCLC hole mobilities up to 8.72 × 10^{-2} cm^2 V^{-1} s^{-1}, amongst the highest reported hole mobility values for solution-processed small-molecule organic semiconductors, are obtained from thermally-annealed device-sized thin films of a thiophene-containing polycyclic aromatic hydrocarbon.

Charge carrier (hole or electron) mobility is one important parameter affecting the performance of organic electronic/optoelectronic devices including organic solar cells.[1] The highest hole mobilities (up to ~45 cm^2 V^{-1} s^{-1}) for organic semiconductors have been demonstrated on macroscopic, highly-ordered, single crystals of conjugated molecules.[2,3] Benefitting from the fast advancement of materials chemistry, the hole mobilities of organic-semiconductor thin films, which are usually prepared by spin-coating or vacuum deposition, have also steadily increased to as high as 12 cm^2 V^{-1} s^{-1}.[4,5] Almost all of these high hole mobility values have been obtained by the field effect transistor (FET) method. Compared to the FET method, which measures the mobility parallel to the electrodes under influence of a gate bias, the space charge limited current (SCLC) method measures the mobility perpendicular to the electrodes.[6] The SCLC mobility is thus more relevant to solar cells. The FET and the SCLC techniques are two of the most widely used methods to investigate charge carrier mobility in organic compounds. The SCLC mobility of organic-semiconductor thin films is often lower by a few orders of magnitude than their FET mobility.[6] Despite a few reports of high SCLC mobilities (up to 1.4 cm^2 V^{-1} s^{-1}) measured in mesoscopic/microscopic areas of discotic liquid crystalline conjugated molecules,[3] the SCLC mobilities of macroscopic organic-semiconductor thin films are generally much lower, ranging from 10^{-6} to 10^{-4} cm^2 V^{-1} s^{-1}.[6–8]

Among myriads of conjugated molecules, polycyclic aromatic hydrocarbons (PAHs) have drawn the most interest and been widely investigated for electronic applications.[9–16] Their often planar or near-planar geometry and extended π-delocalization can induce strong π–π stacking resulting in potentially high charge carrier mobility along the stacked PAH column.[11,15,16] Indeed, the majority of the reported highest SCLC hole mobilities are obtained from PAHs.[2,3] A thiophene-containing fused PAH, namely 2,5,9,12-tetra(*tert*-butyl)diacenaphtho[1,2-*b*:1´,2´-*d*]thiophene (DAT) (**1**) (Fig. 1a), was first synthesized approximately fifteen years ago but has not drawn much attention.[17,18] Nor have its electronic properties/applications been carefully investigated. Herein, we report that spin-coated thin films of this PAH exhibit unusually high SCLC hole mobility after thermal annealing. The peripheral *tert*-butyl groups in **1** prevented π–π stacking during the spin-coating process when solvent was evaporated quickly, resulting in a uniform and amorphous pristine film, which exhibited typical unappealing hole mobility. After thermal annealing, the entire amorphous film became highly crystalline, yielding one of the highest SCLC hole mobilities in organic thin films measured in macroscopic device sizes. For comparison, we also report the thin film hole mobility of a highly twisted PAH, namely 6,7,8,15,16,17-hexaphenyl-1.18,4.5,9.10,13.14-tetrabenzoheptacene (**2**) (Fig. 1b). Thin films of this compound exhibited low crystallinity either before or after thermal annealing, consequently resulting in mediocre hole mobilities in both cases.

Compound **1** was prepared according to a previously published procedure,[17] while compound **2** was prepared using modified literature procedures.[19,20] Their structures and purity have been confirmed by various spectroscopic methods (see the ESI†).

To predict the core geometries and the electronic structures of the two compounds, theoretical calculations were carried out using the density functional theory (DFT) with Gaussian03 at the B3LYP level with the 6-31G(d) basis set. The energy-minimized conformers of the two compounds from different views are shown in Fig. 1c-f. The DAT core of **1** has a near-planar geometry, while that of **2** is highly twisted because of the steric encumbering effect of the six phenyl substituents at bay areas. The calculated end-to-end twist of the heptacene in the approximate D_2-symmetric ground state of **2** is 143.9°. The solid state structure has a twist along the acene of 131.4°, which is lower than the calculated structure probably due to crystal packing forces. The highest occupied molecular orbitals (HOMO) and the lowest unoccupied molecular orbitals (LUMO) of the energy-minimized conformers of **1** and **2** are visualized in Fig. S1 (ESI†), and their energy levels are summarized in Table 1. With calculated HOMO/LUMO energy levels of −5.01/−1.88 eV and −4.71/−2.15 eV, respectively, both **1** and **2** are potentially *p*-type semiconductors.

The UV-vis absorption and fluorescence emission spectra of the two compounds in dilute solutions (black) and as thin films before (red) and after (blue) thermal annealing are depicted in

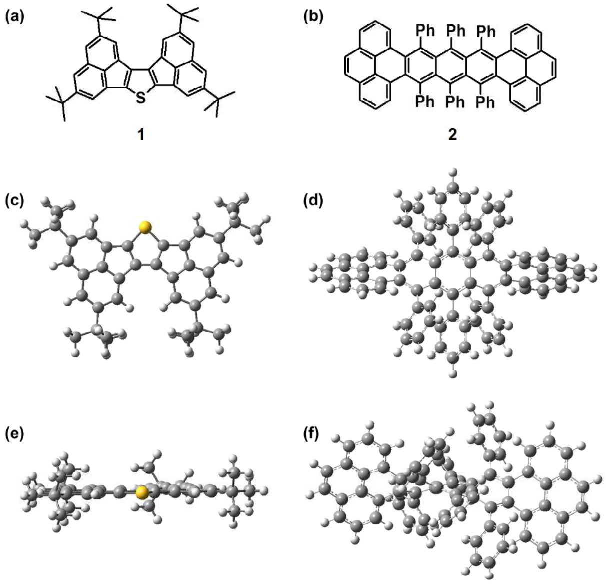

Fig. 1 (a-b) Structures of compounds **1** and **2**. Energy-minimized geometries of **1** (c, e) and **2** (d, f) from different views obtained using DFT calculations at the B3LYP/6-31G(d) level.

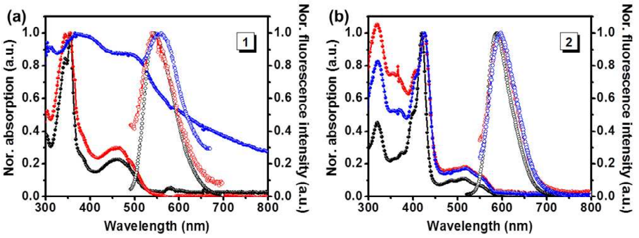

Fig. 2 Normalized UV-vis absorption (spheres) and emission [open circles; excited at 356 nm and 420/426 (solution/film) nm for **1** and **2**, respectively] spectra of (a) **1** and (b) **2** in $CHCl_3$ (black) and as thin films (unannealed: red; annealed: blue).

Fig. 2. Except for a minor change in the relative intensity of the split absorption peaks at 344 and 356 nm, the spin-coated pristine thin film of **1** exhibits essentially the same absorption and emission spectra profiles as those in $CHCl_3$ solution (Fig. 2a). This indicates the lack of effective intermolecular π–π stacking in the pristine thin film. It is presumably due to the steric hindrance induced by the four peripheral *tert*-butyl groups and the fast drying nature of spin-coating $CHCl_3$ solutions. The as-spin-coated thin film of **2** however shows a 4-6 nm red-shift in both the absorption and the emission spectra as compared to its $CHCl_3$ solution (Fig. 2b). This result indicates the existence of some weak or partial intermolecular π–π stacking presumably of the pyrene units. Interestingly, the absorption of the thin film of **1** after thermal annealing (at 120 °C for 10 min) is drastically broadened and red-shifted with emergence of a new, long tail extending to over 800 nm. It is due to a strong intermolecular π–π stacking in the annealed thin film of **1** presumably induced by its near-planar core geometry, which is further confirmed by the broadening and the red-shift (by ~20 nm) of its emission peak. The absorption and emission spectra of thin film **2** however show minimal changes after thermal annealing. Compounds **1** and **2** are weakly fluorescent with quantum yields of 0.0028/0.0029 and 0.0082/0.0086 (in $CHCl_3$/THF), respectively.

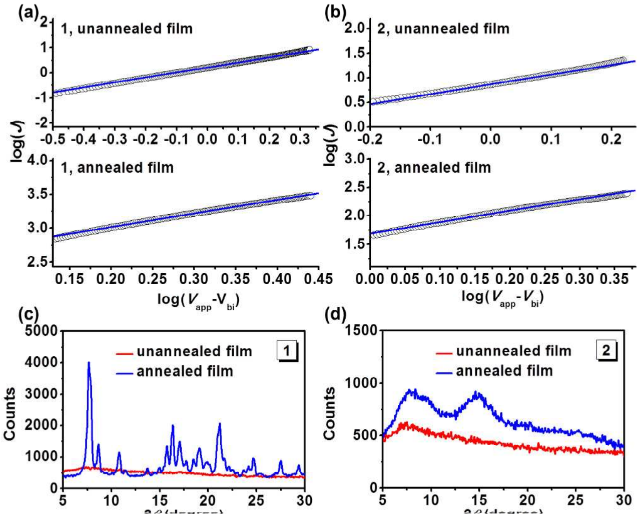

Fig. 3 (a-b) Experimental (black circles) and fitted (blue lines) current density-voltage characteristics of the highest-performing hole-only devices of thin films of **1** and **2** with configuration of ITO/PEDOT:PSS/**1** or **2**/MoO_3/Au with and without thermal annealing. (c-d) XRD patterns of unannealed (red lines) and annealed (blue lines) thin films of **1** and **2**.

The electrochemical properties of the two compounds were investigated as thin films using cyclic voltammetry (CV) measurements. As shown in Fig. S5 (ESI†), these compounds show one or two semi-reversible reduction waves during the cathodic scan and two irreversible oxidation waves in the anodic scan. From the first oxidation onset potential in the anodic scan and the first reduction onset potential in the cathodic scan,[21] the HOMO/LUMO energy levels of **1** and **2** are calculated to be −5.34/−2.68 eV and −5.11/−3.03 eV (Table 1), respectively.

Charge-carrier (hole) mobility of as-spin-coated and thermally annealed thin films of **1** and **2** were measured by the steady-state SCLC technique. Hole-only devices were fabricated with configuration of ITO/PEDOT:PSS/**1** or **2**/MoO_3/Au. The individual active film is of typical organic solar cell device area (0.14 cm^2). The $J-V$ characteristics of the hole-only devices are shown in Fig. 3a-b. Assuming contacts to be ohmic,[22] the hole mobilities in the thin films can be obtained by fitting these $J-V$ curves in the SCLC region using the following equation:[7]

$$J = \frac{9}{8}\varepsilon_0\varepsilon_r\mu\frac{(V_{app}-V_{bi})^2}{d^3} \tag{1}$$

where J is the current density in the SCLC region, V_{app} is the applied voltage, V_{bi} is the built-in voltage, ε_0 is the permittivity of free space (8.854×10^{-12} F/m), ε_r is the relative dielectric constant of the thin film which is assumed to be 3 (a typical value for an organic semiconductor),[7] μ is the charge carrier mobility, and d is the thickness of the thin film which is measured to be in the range of 380~860 nm in the present cases. The derived mobility values are summarized in Table 1. The as-spin-coated thin films of **1** and **2** exhibit hole mobility of 4.61×10^{-5} and 1.05×10^{-4} cm^2 V^{-1} s^{-1} (mean from 10 devices), respectively. The absence of long-range order in the as-spin-coated thin film of **1** was evident in its diffractogram (Fig. 3c), which shows no distinguishable feature. The XRD pattern of as-spin-coated thin film of **2** however shows a broad peak centered at ~7.5° (Fig. 3d). This low-angle peak indicates the presence of randomly ordered lamellar structure in the as-spin-coated thin film of **2**, which can at least partially explain its higher hole mobility than that of **1**. After thermal annealing (at 120 °C for 10 min), the hole mobility of the thin film was elevated to 7.08 × 10^{-2} and 4.53 × 10^{-4} $\mathrm{cm^2\ V^{-1}\ s^{-1}}$ (mean from 10 devices) for **1** and **2**, respectively. The reproducibility of the measured mobility is good from device to device and batch to batch as reflected by the small standard deviation. The highest SCLC hole mobility obtained from the annealed thin films of **1** is 8.72 × 10^{-2} $\mathrm{cm^2\ V^{-1}\ s^{-1}}$ (Table 1), which is amongst the highest reported hole mobilities obtained by either FET or SCLC method for solution-processed small-molecule organic semiconductors.[23,24] The increase of mobility by a factor of more than three orders of magnitude for **1** upon thermal annealing is attributed to its drastically increased crystallinity and long-range order as revealed by the sharp intense peaks in the XRD pattern of the thin film after thermal annealing (Fig. 3c).[25] Thermal annealing also increased the hole mobility of **2** by a factor of ~4.2. The intensity of the broad peak (at ~7.5°) increased and a new broad peak (at ~14.6°) appeared, indicating some increase of crystallinity and the number of ordered lamellar structures in the annealed film of **2**.[26] Restraint by the highly twisted geometry, the enhancement of crystallinity in **2** upon thermal annealing is not as drastic as that in **1** (Fig. 3d). These results are all consistent with the optical studies.

Table 1 Experimental and calculated frontier energy levels and SCLC hole mobilities of the compounds

Compound	Experimental[a]			Calculated[b]			$\mu_h/(\mathrm{cm^2\ V^{-1}\ s^{-1}})$[c,d]	
	E_{HOMO}/eV	E_{LUMO}/eV	E_g/eV	E_{HOMO}/eV	E_{LUMO}/eV	E_g/eV	Unannealed	Annealed[e]
1	−5.34	−2.68	2.66	−5.01	−1.88	3.13	$4.61 \pm 3.18 \times 10^{-5}$ (1.10×10^{-4})	$7.11 \pm 1.06 \times 10^{-2}$ (8.72×10^{-2})
2	−5.11	−3.03	2.08	−4.71	−2.15	2.56	$1.05 \pm 0.7 \times 10^{-4}$ (2.41×10^{-4})	$4.53 \pm 2.23 \times 10^{-4}$ (8.89×10^{-4})

[a] From CV measurement of thin solid film. [b] Using DFT calculations at the B3LYP/6-31G(d) level. [c] Mean SCLC mobility with standard deviation from 10 devices of at least two batches for each fabrication condition. [d] The value in parentheses is the highest SCLC mobility observed. [e] Thermally annealed at 120 °C for 10 min.

In summary, we report the optical, electrochemical, crystallinity properties and hole mobilities of a thiophene-containing fused PAH **1**, and a highly twisted PAH **2**. DFT calculations reveal a near-planar core-geometry for **1** and a highly twisted structure for **2** with a heptacene end-to-end twist of 143.9°. The pristine thin films of **1** and **2** fabricated by spin-coating process show average hole mobility of 4.35 × 10^{-5} and 1.08 × 10^{-4} $\mathrm{cm^2\ V^{-1}\ s^{-1}}$, respectively. Thermal annealing led to broadened and red-shifted absorption and emissions with improved hole mobility by over three orders of magnitude to as high as 8.72 × 10^{-2} $\mathrm{cm^2\ V^{-1}\ s^{-1}}$. This result is amongst the highest reported hole mobilities obtained by either FET or SCLC method for solution-processed small-molecule organic semiconductors. The difference in the core structure for the two compounds is one of sterics, specifically, the phenyl groups that do not allow the heptacene core to exist in a planar structure. This twisted structure inhibits π–π stacking along the core as well as the pyrene end caps. On the other hand, the thiophene core is planar even with the *tert*-butyl groups on the acenaphthene units. While these groups increase the solubility, they do not allow for an ordered thin film upon initial deposition resulting in random orientations of the molecules. The annealing of the thin film allows for the reorganization and ordering of the individual molecules. Therefore, the enhancement in hole mobility of **1** is attributed to the drastically increased crystallinity and long-range order induced by strong intermolecular π–π stacking upon thermal annealing. These discoveries may help guide the rational design of new highly-performing organic photovoltaic materials. A detailed study to explore the effect of peripheral substituents of different type and size on the hole mobilities of the resulting DAT derivatives has been initialized.

This research was supported by the National Science Foundation (DMR1308577), Army Research Office (W911NF-10-1-0476), and the University of Missouri-Kansas City.

Notes and references

[a] *Department of Chemistry, University of Missouri-Kansas City, Kansas City, Missouri 64110, United States. E-mail: pengz@umkc.edu; kilwayk@umkc.edu*

† Electronic Supplementary Information (ESI) available: Experimental details; synthesis and characterization of **1** and **2**; visualized LUMO+1, LUMO, HOMO and HOMO−1 orbitals of the energy-minimized conformers; UV-vis absorption and florescence emission spectra; cyclic voltammograms; DSC thermograms. See DOI: 10.1039/b000000x/

1 A. J. Heeger, *Adv. Mater.*, 2014, **26**, 10.
2 (*a*) V. C. Sundar, J. Zaumseil, V. Podzorov, E. Menard, R. L. Willett, T. Someya, M. E. Gershenson and J. A. Rogers, *Science*, 2004, **303**, 1644; (*b*) O. D. Jurchescu, M. Popinciuc, B. J. van Wees and T. T. M. Palstra, *Adv. Mater.*, 2007, **19**, 688; (*c*) J. Takeya, M. Yamagishi, Y. Tominari, R. Hirahara, Y. Nakazawa, T. Nishikawa, T. Kawase, T. Shimoda and S. Ogawa, *Appl. Phys. Lett.*, 2007, **90**, 102120; (*d*) W. Xie, K. A. McGarry, F. Liu, Y. Wu, P. P. Ruden, C. J. Douglas and C. D. Frisbie, *J. Phys. Chem. C*, 2013, **117**, 11522.
3 E. M. García-Frutos, U. K. Pandey, R. Termine, A. Omenat, J. Barberá, J. L. Serrano, A. Golemme and B. Gómez-Lor, *Angew. Chem. Int. Ed.*, 2011, **50**, 7399.
4 M. H. Hoang, Y. Kim, M. Kim, K. H. Kim, T. W. Lee, D. N. Nguyen, S.-J. Kim, K. Lee, S. J. Lee and D. H. Choi, *Adv. Mater.*, 2012, **24**, 5363.
5 I. Kang, H.-J. Yun, D. S. Chung, S.-K. Kwon, Y.-H. Kim, *J. Am. Chem. Soc.*, 2013, **135**, 14896.
6 B. C. Thompson, B. J. Kim, D. F. Kavulak, K. Sivula, C. Mauldin and J. M. J. Fréchet, *Macromolecules*, 2007, **40**, 7425.
7 L. Zhang, X. Xing, Z. Chen, L. Xiao, B. Qu and Q. Gong, *Energy Technol.*, 2013, **1**, 613.
8 T.-Y. Chu and O.-K. Song, *Appl. Phys. Lett.*, 2007, **90**, 203512.
9 B. R. Kaafarani, *Chem. Mater.*, 2011, **23**, 378.
10 A. Bayn, X. Feng, K. Müllen and H. Haick, *ACS Appl. Mater. Interfaces*, 2013, **5**, 3431.
11 W. W. H. Wong, C.-Q. Ma, W. Pisula, C. Yan, X. Feng, D. J. Jones, K. Müllen, R. A. J. Janssen, P. Bäuerle and A. B. Holmes, *Chem. Mater.*, 2010, **22**, 457.
12 C. B. Nielsen, R. S. Ashraf, B. C. Schroeder, P. D'Angelo, S. E. Watkins, K. Song, T. D. Anthopoulos and I. McCulloch, *Chem. Commun.*, 2012, **48**, 5832.
13 Y. Li, Y. Bian, M. Yan, P. S. Thapaliya, D. Johns, X. Yan, D. Galipeau and J. Jiang, *J. Mater. Chem.*, 2011, **21**, 11131.
14 T. Dutta, Y. Li, A. L. Thornton, D.-M. Zhu and Z. Peng, *J. Polym. Sci., Part A: Polym. Chem.*, 2013, **51**, 3818.

15 L. Schmidt-Mende, A. Fechtenkötter, K. Müllen, E. Moons, R. H. Friend and J. D. MacKenzie, *Science*, 2001, **293**, 1119.
16 X. Feng, V. Marcon, W. Pisula, M. R. Hansen, J. Kirkpatrick, F. Grozema, D. Andrienko, K. Kremer and K. Müllen, *Nature Mater.*, 2009, **8**, 421.
17 J. A. Watson Jr., R. A. Pascal Jr., D. M. Ho and K. V. Kilway, *Tetrahedron Lett.*, 2000, **41**, 5005.
18 K. V. Kilway, K. A. Lindgren, J. A. Watson Jr., R. G. Clevenger, R. D. Ingalls, D. M. Ho and R. A. Pascal Jr., *Tetrahedron*, 2004, **60**, 2433.
19 S. Mondal, A. J. Bhattacharya, *Curr. Sci.*, 1984, **53**, 1229.
20 K. Kitazawa, T. Kochi, M. Sato and F. Kakiuchi, *Org. Lett.*, 2009, **11**, 1951.
21 Y. Li, P. Lu, X. Yan, L. Jin and Z. Peng, *RSC Adv.*, 2013, **3**, 545.
22 On the basis of the measured HOMO energy levels of the compounds and the work functions of PEDOT:PSS (−5.0 eV) and MoO_3 (−5.4 eV).
23 B. Walker, C. Kim and T.-Q. Nguyen, *Chem. Mater.*, 2011, **23**, 470.
24 Y. Sun, G. C. Welch, W. L. Leong, C. J. Takacs, G. C. Bazan and A. J. Heeger, *Nature Mater.*, 2012, **11**, 44.
25 J. Liu, R. Zhang, G. Sauvé, T. Kowalewski and R. D. McCullough, *J. Am. Chem. Soc.*, 2008, **130**, 13167.
26 G. D. Sharma, D. Daphnomili, S. Biswas and A. G. Coutsolelos, *Org. Electron.*, 2013, **14**, 1811.

Table of Contents

Unusually high SCLC hole mobility in solution-processed thin films of a polycyclic thiophene-based small-molecule semiconductor

Yong Li, Robert G. Clevenger, Lu Jin, Kathleen V. Kilway and Zhonghua Peng

Solution-processed thin films of a thiophene-containing polycyclic aromatic hydrocarbon shows SCLC hole mobilities up to 8.72×10^{-2} cm^2 V^{-1} s^{-1}.